Designer self-assembling peptide nanofiber biological materials

Charlotte A. E. Hauser[a] and Shuguang Zhang[ab]

Received 22nd October 2009, Accepted 15th March 2010
First published as an Advance Article on the web 3rd June 2010
DOI: 10.1039/b921448h

Scientists and bioengineers have dreamed of designing materials from the bottom up with the finest detail and ultimate control at the single molecular level. The discovery of a class of self-assembling peptides that spontaneously undergo self-organization into well-ordered structures opened a new avenue for molecular fabrication of biological materials. Since this discovery, diverse classes of short peptides have been invented with broad applications, including 3D tissue cell culture, reparative and regenerative medicine, tissue engineering, slow drug release and medical device development. Molecular design of new materials using short peptides is poised to become increasingly important in biomedical research, biomedical technology and medicine, and is covered in this *tutorial review*.

Introduction

There exists an important a distinction between biomaterials and biological materials. The term "biomaterials" typically refers to the materials now commonly used in medical applications and includes titanium metal, ceramic implants, polymer and biopolymer scaffolds as well as a variety of composites. On the other hand, the term "biological materials" refers to those materials with biological origin, including collagen, fibrin, silk, spider-silk, hair, fur, leather, natural bio-adhesive, shells, cellulose, natural plant oil and a variety of biological surfactants. After decades of fine-tuning, many biological materials can now be designed and fabricated at the molecular level for particular uses. Because of their chemical complexity and structural sophistication, biological materials of natural origin have been more difficult to design and fabricate at the molecular level. However, this has changed over the last two decades.

For a few decades, chemical scientists, chemical engineers, materials scientists and medical doctors have made great efforts to develop a wide range of biomaterials for medical applications. Although most of the materials used in these applications were not specifically designed and made for medical uses, they have nevertheless saved people's lives, alleviated medical problems, and generally improved patients' quality of life while having a profound impact on medical technology.

Because biomaterials are not specifically designed for medical uses, they have shortcomings and sometimes cause

[a] *Institute of Bioengineering and Nanotechnology, A*STAR, 31 Biopolis Way, The Nanos, 138669 Singapore. E-mail: chauser@ibn.a-star.edu.sg; Fax: +65-6478-9080; Tel: +65-6824-7108*
[b] *Center for Biomedical Engineering NE47-379, Massachusetts Institute of Technology, 77 Massachusetts Avenue, Cambridge, MA 02139, USA. E-mail: shuguang@mit.edu; Fax: +1-617-258-5239; Tel: +1-617-258-7514*

Charlotte A. E. Hauser

Charlotte Hauser is a Team Leader and Principal Research Scientist at the Institute of Bioengineering and Nanotechnology (IBN) in Singapore. She did her PhD studies at the Massachusetts Institute of Technology (MIT), Cambridge, USA. She was a Research Fellow at the Institute National de la Santé et de la Recherche Médicale (INSERM) in Paris, France, and led a research group at the Max-Planck-Institute (MPI) of Psychiatry in Munich, Germany. She founded life science company Octagene, Martinsried, Germany, now with Octapharma AG, and was managing director and shareholder (1997–2006). She holds numerous scientific articles, patents and received many awards and prizes.

Shuguang Zhang

Zhang Shuguang earned his PhD in Biochemistry & Molecular Biology from University of California at Santa Barbara. He has published >140 papers in protein science and nanobiotechnology from designer self-assembling peptides, study membrane proteins to emerging biosolar energy. He was an American Cancer Society Postdoctoral Fellow and a Whitaker Foundation Investigator at MIT. He is a distinguished Chang Jiang scholar in China and a 2003 Fellow of Japan Society for Promotion of Science. His work on designer peptide scaffolds won 2004 R&D100 award. He was a 2006 John Simon Guggenheim Fellow and a winner of 2006 Wilhelm Exner Medal of Austria. He was inducted as a foreign member of the Austrian Academy of Science in 2010.

problems. However, the benefits out-weight the risks and they continue to be used today.

Since biomaterials are not ideal for all medical applications, scientists and engineers are turning their attentions to the development of biological materials, namely, materials of biological origin including collagen, fibrin, silk, spider-silk, hair, fur, leather, natural bio-adhesive, shells, cellulose, natural oil and a variety of biological surfactants. The advent of molecular biology and biotechnology has accelerated this trend. Inspired by nature, more and more biological materials have been developed during the last decade, a trend that is expected to continue. It should not be surprising if, in the future, biological materials eventually supersede biomaterials for medical uses.

In order to design biological materials for particular uses, or "tailor-made biological materials", it is absolutely essential to understand their finite, nature-made, individual building blocks. These building blocks include the twenty natural L-amino acids, tens of natural lipids, tens of sugars and a few nucleotides.

We began conducting biological material research in the early 1990s after serendipitously discovering a self-assembling peptide, EAK16, that self-organized into ordered nanofibers and further into scaffolds. This discovery was made while working on yeast genetics and structural biology in the laboratory of Alexander Rich at the Massachusetts Institute of Technology. This unexpected discovery led a new way of thinking about how to design a variety of biological materials from the bottom up. This new approach allows exquisite fine-tuning and the ability to control one amino acid at a time, thus laying a foundation for the design of a wide spectrum of biological materials and medical devices.

This field is advancing rapidly as more and more people from biology, chemistry and various engineering areas enter and new reports come out daily, making it impossible to cover the entire field within a few limited pages. We will therefore only focus on our own research highlights in this review and invite interested readers to consult the original reports and early reviews in the literature for a more comprehensive view.

Discovery of the first self-assembling peptide, EAK16, in baker's yeast

In science, it is crucial not only to make careful and repeatable observations, but also to carry out reproducible experiments. When one observes an unusual phenomenon and cannot interpret it using conventional theories, one should consider the alternatives. Many discoveries are made unintentionally and serendipitously, sometimes referred to as unauthorized scientific discoveries, while one works in a specific area but accidentally discovers something else in a completely unrelated area. The discovery of self-assembling peptides is one such example, thus justifying curiosity-driven and broad basic research.

We both worked in Alexander Rich's laboratory from the late 1980s to early 1990s to gain understanding of the biological function of left-handed Z-DNA binding protein. While working on yeast genetics and protein chemistry in 1989, one of us, Shuguang Zhang, identified a protein that he named zuotin (*zuo means left in Chinese*, *tin refers to protein in this case*) for its ability to bind to left-handed Z-DNA in the presence of 400-fold excess of sheared salmon DNA, which contains ubiquitous right-handed B-DNA and other DNA structures.[1] Zuotin had an interesting repetitive 16-residue peptide sequence motif, n-AEAEAKAKAEAEAKAK-c (EAK16-II), among a segment of alternating alanine-X repeating 34 residues.[1,2] Out of curiosity, Zhang custom-made this peptide to study its biochemical and structural properties. To our great surprise, the results of almost everything we studied were different from what was known in the literature at the time. This aroused our curiosity further, and we persistently pursued this discovery. Since then this peptide sequence has been extensively studied to create a class of simple β-sheet peptides.[3]

These peptides are ionic self-complementary as a result of the presence of both positive and negative side chains on one side of the β-sheet and hydrophobic side chains on the other (Fig. 1). These peptides have two distinctive sides, one hydrophobic and the other hydrophilic. The hydrophobic side forms a double sheet inside of a fiber and the hydrophilic side forms the outside of the nanofibers that interact with water molecules, forming an extremely high water content hydrogel, which can contain as high as 99.5% to 99.9% water (1–5 mg peptide per ml water, w/v). At least three types of molecules can be made, with −, +, −/+ on the hydrophilic side (Fig. 1).[4]

This serendipitous discovery of a self-complementary peptide inspired us to design many more members of this class of

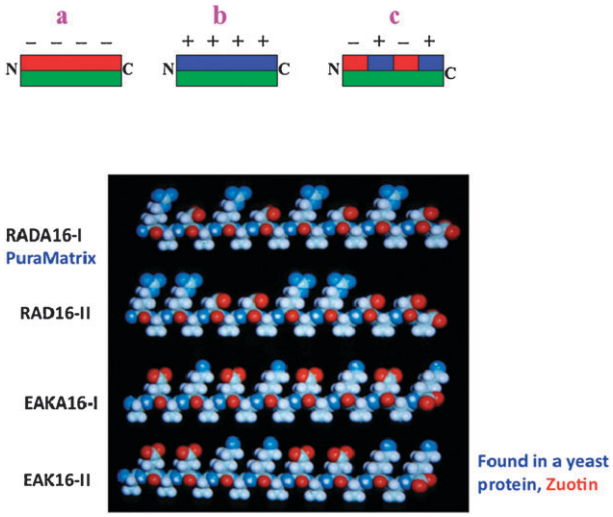

Fig. 1 The simple and molecular models of the designer amphiphilic self-assembling peptides that form well-ordered nanofibers. (Upper Panel) These peptides have two distinctive sides, one hydrophobic and the other hydrophilic. The hydrophobic side forms a double sheet inside of the fiber and the hydrophilic side forms the outside of the nanofibers that interact with water molecules, forming an extremely high water content hydrogel that contains as high as 99.9% water. At least three types of molecules can be made, with −, +, −/+ on the hydrophilic side. (Lower Panel) The individual self-assembling peptide molecules are ~5 nm long. The first such peptide, EAK16-II, was discovered from a yeast protein, zuotin.[1,2] This peptide inspired us to design a large class of self-assembling peptide construction motifs. When dissolved in water in the presence of salt, they spontaneously assemble into well-ordered nanofibers and then further into scaffolds (for more details, see Fig. 2–7).

peptides, which form 3-dimensional (3D) nanofiber scaffolds that have been used in 3D cell tissue cultures.[5–9] The 4 ionic self-complementary peptides (Fig. 1 - lower panel) RADA16-I, RAD16-II, EAK-I and EAK16-II (the segment from yeast zuotin) form stable β-sheet structures in water and undergo spontaneous assembly to form nanofiber scaffolds. The nanofiber scaffolds hold large volumes of water since water molecules can perhaps be organized through surface tension to form clusters divided by nanofibers into compartments. Tissue cells can be embedded in such a 3D nanofiber scaffold[5–9] in which they can establish molecular gradients that often mimic the *in vivo* environment.

Other related self-assembling peptide systems have also been designed, which range from 'molecular switch' peptides that undergo marked conformational changes[10,11] to 'molecular ink' peptides for surface engineering[12] to peptide surfactants that self-assemble into micelles, nanotubes and nanovesicles,[13–19] all of which were inspired by the Z-DNA-binding zuotin discovery. But these findings will not be covered in this review.

The chemical properties of the self-assembling peptide systems

The self-assembling peptide scaffolds consist of alternating amino acids that contain 50% charged residues.[3–9,20–25] These peptides are characterized by their periodic repeats of alternating ionic hydrophilic and hydrophobic amino acids with a typical β-sheet structure. Thus, these β-sheet peptides have distinct polar and non-polar surfaces (Fig. 1). The self-assembly event that creates the peptide scaffold takes place under physiological conditions of neutral pH and millimolar salt concentration. They are like gel-sponges in aqueous solution, not only readily transportable to different environments but also injectable through the smallest needles. Individual hydrated fibers are $\sim$10 nanometres in diameter. A number of additional designer self-assembling peptides including RADA16-I (AcN-RADARADARADARADA-CNH_2) and RADA16-II (AcN-RARADADARARADADA-CNH_2) have been designed, in which arginine and aspartate residues replace the lysine and glutamate residues of the EAK peptides. The alanines form overlapping hydrophobic interactions in water, making a structure that is found in silk fibroin from silkworm and spider silk.[26] On the charged sides, both positive and negative charges are packed together through intermolecular ionic interactions in a checkerboard-like manner. In general, these self-assembling peptides form stable β-sheet structures in water, which are stable at high temperatures, across a wide pH range, and in the presence of a high concentration of denaturing agents urea and guanidium hydrochloride.[3] The nanofiber density correlates with the concentration of peptide solution, and the nanofibers retain extremely high hydration, >99% in water (1–10 mg ml^{-1}, w/v) (Fig. 3).

Commercial peptide synthesis methods use conventional solid phase or solution peptide synthesis chemistry. Depending on the length of the motifs, high purity peptides can be produced at a reasonable cost. The cost of peptide synthesis has steadily decreased in recent years, making it more and more affordable. However, it is still expensive for wide spread use and further cost reduction is necessary. It is now possible to produce some peptides as multiple cleavable units in a bacterial system, which will further reduce the cost of synthesis.

Many self-assembling peptides that form scaffolds have been reported and the numbers are still expanding.[4,23] The formation of the scaffold and its mechanical properties are influenced by several factors, one of which is the level of hydrophobicity.[20,22,24] That is, in addition to the ionic complementary interactions, the content of hydrophobic residues, Ala, Val, Ile, Leu, Tyr, Phe, Trp (or single letter code, A, V, I, L, Y, P, W) can significantly influence the mechanical properties of the scaffolds and the speed of their self-assembly. The higher the content of hydrophobicity, the easier it is for nanofiber scaffold formation and better mechanical property strength.[20,22,24,25]

Self-assembling peptide nanofiber scaffolds

A hierarchical scaffold self-organization starting from a single molecule of the ionic self-complementary peptide RADA16-I is depicted in Fig. 2. Here millions of peptide molecules self-assemble into individual nanofibers, and billions of nanofiber further self-assemble into the nanofiber scaffold (Fig. 2). The nanopores in the scaffold range from a few nanometres to a few hundred nanometres. The nanopores are similar in size to most biomolecules, so that these molecules, either small molecule drugs or protein and nucleic acid therapeutics, may not only defuse slowly but also may establish a molecular gradient in the nanoporous scaffolds.

Peptide samples in aqueous solution were examined using environmental AFM and showed nanofiber results, thus suggesting the nanofiber formation is independent of the drying process (Fig. 2 - lower panel).

It is interesting to observe that at high resolution the nanofibers appear to have distinct layers, especially in some segments (Fig. 3). The difference in height is $\sim$1.4 nm, which is similar to the thickness of a single peptide. Fig. 3e–h shows the peptide scaffold hydrogel at various concentrations, 0.6–3 mM, (1–5 mg ml^{-1}, w/v, or 99.5–99.9% water content).[2–9] The scaffold hydrogel is completely transparent, which is a very important requirement for accurate image collection in applications using 3-D tissue cell cultures.

Dynamic reassembly of self-assembling peptides

The self-assembling peptides form a stable β-sheet structure in water (Fig. 4). The interactions between the peptides and β-sheets are (1) non-covalent hydrogen bonds along the backbones, (2) the arrays of ionic + and − charge interactions, (3) alanine hydrophobic interactions and van der Waals interactions, and (4) water-mediated hydrogen bond formations. Thus the nanofibers can be disrupted mechanically using sonication.[25] The self-assembling process is reversible and dynamic (Fig. 5) since these peptides are short and simple. Numerous individual peptides can be readily self-organized through the weak interactions. However, they can undergo dynamic reassembly repeatedly (Fig. 4), similar to the material self-healing process. Since the driving energy of the assembly in water is not only through hydrophobic van der Waals

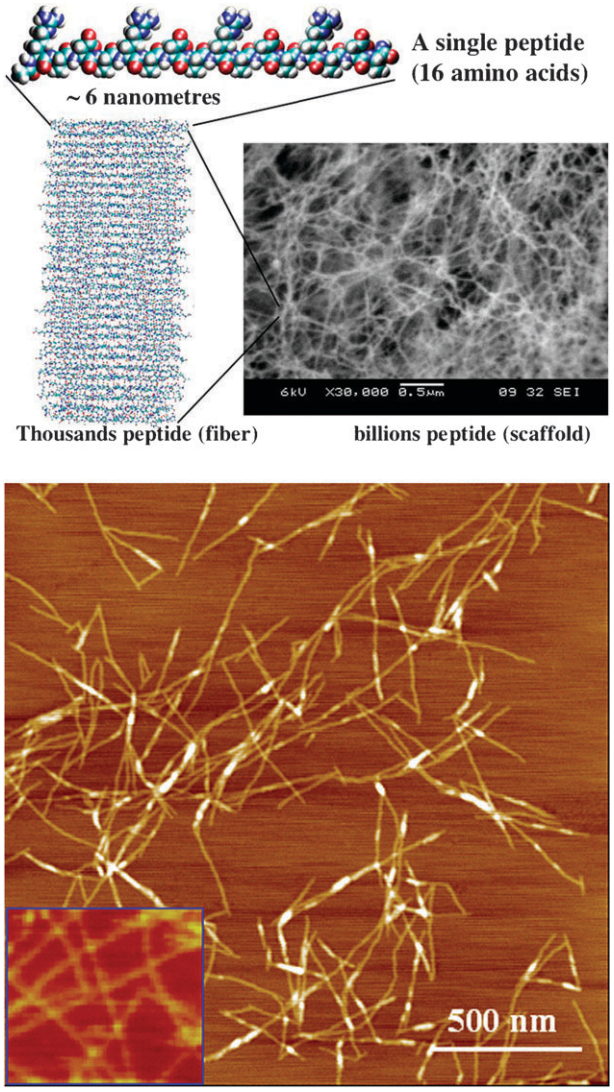

Fig. 2 Self-assembling peptide RADA16-I nanofiber scaffold hydrogel. (Upper panel) Amino acid sequence of RADA16-I, molecular model of a single RADA16-I nanofiber, the calculated peptide dimensions are ~6 nm long depending on end capping, 1.3 nm wide and 0.8 nm thick; tens and hundreds of thousands of individual peptides self-assemble into a nanofiber, SEM images of RADA16-I nanofiber scaffold. Note the scale bar, 0.5 μm or 500 nm (SEM image courtesy of Fabrizio Gelain). (Lower panel) RADA16-I Peptide form nanofibers in aqueous solution that further form hydrogel with extremely high water content (99.5–99.9% w/v water). Peptide samples in aqueous solution using environmental AFM examination showed the same nanofiber results (the insert at bottom left) suggesting that the nanofiber formation is independent of the air-drying process. The nanofiber images however are not as sharp as the ones dried on mica, likely due to the hydration of these nanofibers in solution.

interactions, but also the arrays of ionic interactions as well as the peptide backbone hydrogen bonds, this phenomenon can be further exploited for production and fabrication of many self-assembling peptide materials.

Unlike processed polymer microfibers in which the fragments of polymers cannot undergo reassembly without addition of catalysts or through material processing, the supramolecular

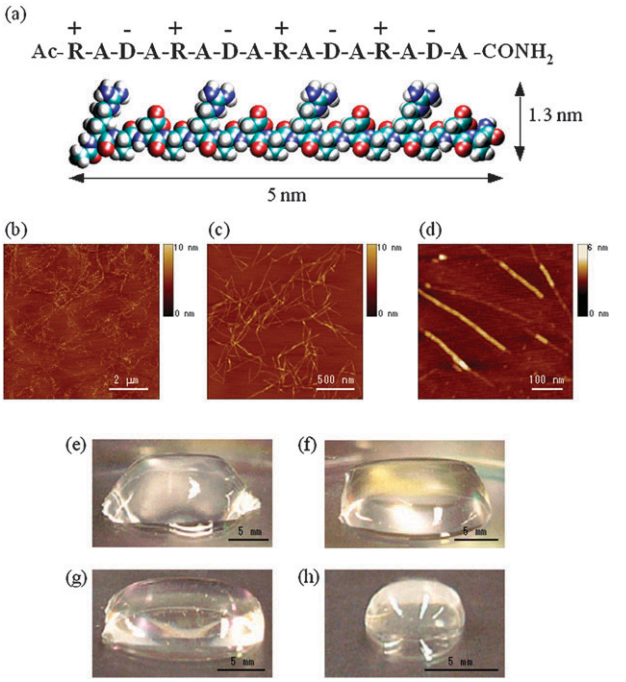

Fig. 3 Peptide RADA16-I. (a) Amino acid sequence and molecular model of RADA16-I, the dimensions are ~5 nm long, 1.3 nm wide and 0.8 nm thick. AFM images of RADA16-I nanofiber scaffold, (b) 8 μm^2, (c) 2 μm^2 (d) 0.5 μm^2. Note the different height of the nanofiber, ~1.3 nm, in (d) suggesting a double layer structure; Photographs of RADA16-I hydrogel at various conditions, (e) 0.5 wt% (pH 7.5), (f) 0.1 wt% (pH 7.5, Tris.HCl), (g) 0.1 wt% (pH 7.5, PBS) before sonication, (h) re-assembled RADA16-I hydrogel after 4 times of sonication, respectively (image courtesy of Hidenori Yokoi).

self-assembly and reassembly event is likely to be wide spread in many unrelated fibrous biological materials where numerous weak interactions are involved. Self-assembly and reassembly are a very important property for fabricating novel materials, and it is necessary to fully understand its detailed process in order to design and to improve biological materials.

AFM images reveal that the nanofibers range from several hundred nanometres to a few microns in length before sonication. After sonication, the fragments were broken into ~20–100 nanometres. The kinetics of the nanofiber reassembly is examined closely at 1, 2, 4, 8, 16, 32 and 64 min as well as 2, 4, and 24 h (Fig. 4). The nanofiber length reassembly is a function of time: by 2 h, the peptide nanofibers have essentially reassembled to their original length. The CD spectra showed little change since the β-sheets at the molecular level remain unchanged despite the nanofiber length change.

This remarkable reassembly is interesting because there may be a small amount of nucleation for re-growth of the nanofiber from the addition of monomers that may be produced during sonication. It is plausible that a large population of the sonicated nanofiber fragments contains many overlapping cohesive ends due to the undisrupted alanine hydrophobic side that may quickly find each other (Fig. 5). The situation is analogous and commonly found in sonicated and enzymatic digested DNA restriction fragments that can find each other to re-align the ends as a function of time.

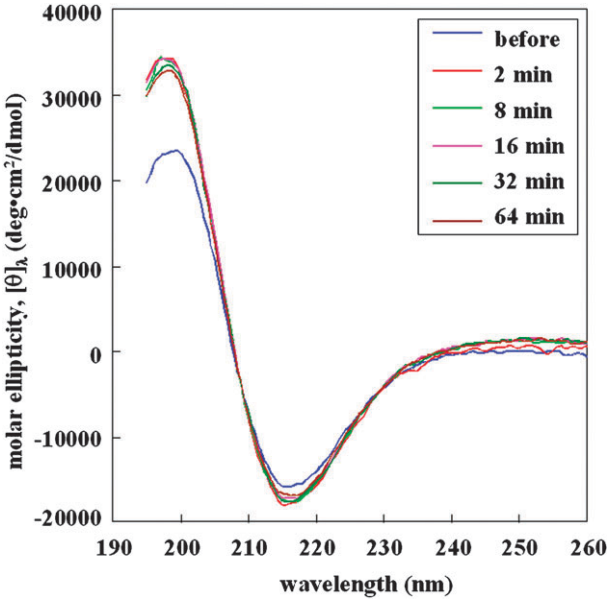

Fig. 4 Circular dichroism examination of the peptide structures at various times before and after sonication. Before indicates sample taken before sonication; sample time points 2, 8, 16, 32, 64 min were taken after sonication. The typical β-sheet spectra were observed at all time point experiments indicating the molecular structure and the integrity of the peptides were unchanged before and after sonication. Furthermore, the β-sheet contents (216 nm) remain nearly identical at all time points and slight higher than the sample before sonication suggesting tight β-sheet packing. However, the degree of β-sheet twist (195 nm region) before sonication is different suggesting different β-sheet packing. It is possible that the sonication and reassembly process further facilitated packing (image courtesy of Hidenori Yokoi).

Chiral self-assembling peptides made of all D-amino acids

Numerous self-assembling peptides with various compositions, sequences, and length have been studied, largely using peptides composed of L-amino acids. We also wonder if the chiral peptides made of all D-amino acids can also undergo self-assembly and form nanofiber, similar to their L-peptide counterparts. Since D-form peptide bonds resist natural L-enzyme degradation, D-peptide based materials will likely be more stable. Thus, a new class of D-form self-assembling peptides may prove to be more versatile in fabricating novel supramolecular architecture and have a wide range of applications in biotechnology, nanobiotechnology and medical technology.

Luo Zhongli and his colleagues found that the D-peptide d-EAK16-II forms stable β-sheets with the exact inverted CD spectrum (Fig. 6) as l-EAK16-II.[27,28] They also form well-ordered nanofibers that are structurally indistinguishable from the L-peptide counterpart (Fig. 7).[27,28] They used a pair of identical sequences to undertake the study. The chiral D-form amino acids were used to produce peptides with only D-amino acids. They showed that the D-peptides have inverted circular dichroism spectra, mirror images of the L-peptides of identical sequence.[27,28] The β-sheet structure of D-peptide is less stable than the L-peptide's at high temperature, ~80 °C and D-peptide can undergo secondary structural transition from β-sheet to α-helix. This raises the very intriguing question

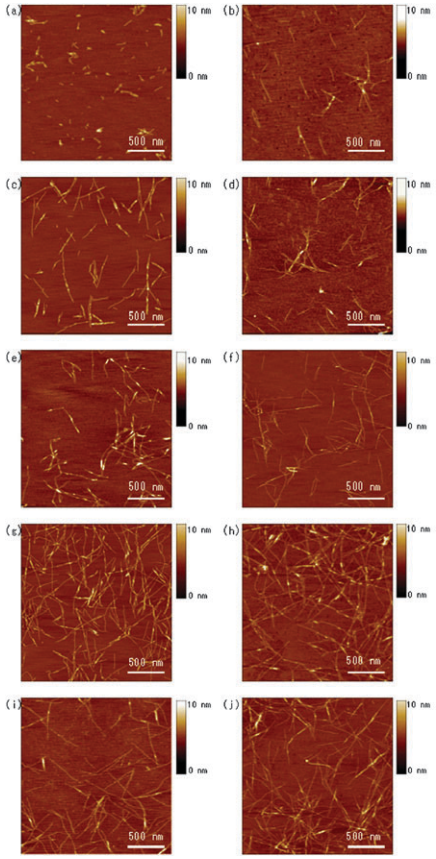

Fig. 5 AFM images of RADA16-I nanofiber at various time points after sonication. The observations were made using AFM immediately after sample preparation. (a) 1 min after sonication; (b) 2 min; (c) 4 min; (d) 8 min; (e) 16 min; (f) 32 min; (g) 64 min; (h) 2 h; (i) 4 h; (j) 24 h. Note the elongation and reassembly of the peptide nanofibers over time. By ~1–2 h, these self-assembling peptide nanofibers have nearly fully re-assembled (image courtesy of Hidenori Yokoi).

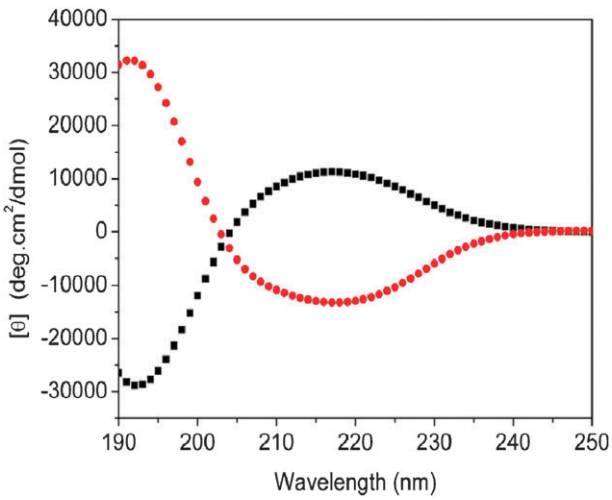

Fig. 6 CD spectra of peptides d-EAK16 (black dots) and l-EAK16 (red dots) in water at 25 °C. The *X*-axis is wavelength in nm; the *Y*-axis is expressed as mole residue ellipticity [*θ*]. The mirror image of d-EAK16 and l-EAK16 reflects the chirality (image courtesy of Zhouli Luo).

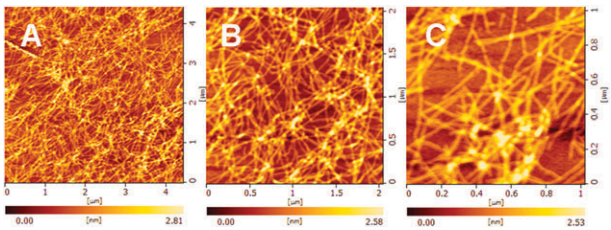

Fig. 7 AFM images of D-chiral peptide d-EAK16 self-assembling into nanofibers (2 mg/ml or 0.2% w/v). The images were systematically collected with increasing magnification. The areas are (A) 4.3 μm^2, (B) 2 μm^2, and (C) 1 μm^2. The well-ordered nanofibers and their pores are clearly visible. The diameter of the nanofibers is about ~10 nm perhaps due to hydration and AFM tip measurement. These images are similar to l-EAK16 reported previously[2] (image courtesy of Zhouli Luo).

of why nature selected L-amino acids for all living systems on Earth. However, the nanofibers and scaffolds formed from the peptides with only D-amino acids are indistinguishable from their L-counterpart.[27,28]

Kinetics of nanofiber reassembly and a plausible reassembly process

The reassembly kinetics is a function of time. It may be similar to DNA reassembly; the re-assembly largely depends on the concentrations of the short complementary fragments. In this case, the fragments are the sonicated peptide nanofibers and possibly sonicated monomers.

In order to understand the dynamics of reassembly, based on reproducible observations, we proposed a plausible sliding diffusion molecular model to interpret these observations of reassembly of the self-assembling RADA16-I peptides (Fig. 8). Unlike the left-handed super-helical structures observed in a different self-assembling peptide KFE8,[24] no super-helical structures were observed for RADA16-I using AFM[25] and SEM.[6,7,21]

Molecular modeling of the self-assembly process

For molecular modeling clarity, the RADA16-I β-sheet is presented as a non-twisted strand. It is known that these peptides form stable β-sheet structures in water, thus they not only show intermolecular hydrogen bonding on the peptide backbones, but they also have two distinctive sides, one hydrophobic with an array of overlapping alanines (Fig. 8, green color sandwiched inside), similar to what is found in silk fibroin or spider silk assemblies.[26] The other side of the backbones have negatively charged (−) amino acids, represented as red, and positively charged (+) amino acids, represented as blue.

The alanines form packed hydrophobic interactions in water, which can be disrupted mechanically during sonication. However, these hydrophobic cohesive ends can find each other quickly in water since the exposure of hydrophobic alanine arrays to water is energetically unfavorable. Since the hydrophobic alanines' interaction is non-specific, they can slide diffuse along the nanofiber, like trains sliding along train tracks. The same sliding diffusion phenomenon was also observed

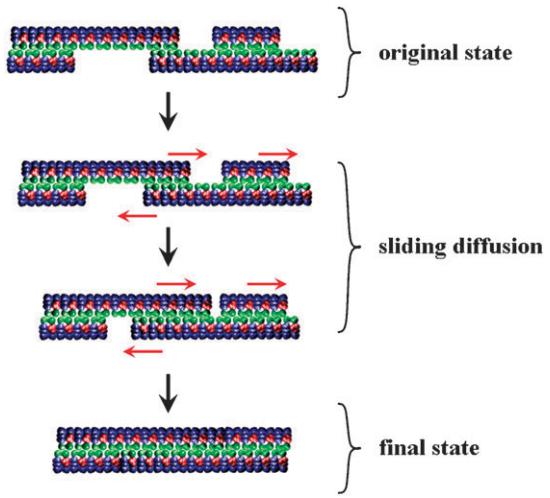

Fig. 8 A proposed molecular sliding diffusion model for dynamic reassembly of a single peptide nanofiber consisting of thousands of individual peptides. When the peptides self-assemble into stable β-sheets in water, they form intermolecular hydrogen bonds along the peptide backbones. The β-sheet structure has two distinctive sides, one hydrophobic with an array of alanines and the other with negatively charged and positively charged amino acids. These peptides form antiparallel β-sheet structures. The alanines form overlap packed hydrophobic interactions in water, a structure that is found in silk fibroin from silkworm and spiders. On the charged sides, both positive and negative charges are packed together through intermolecular ionic interactions in a checkerboard-like manner. When the fragments of nanofiber first meet, the hydrophobic sides may not fit perfectly but have gaps. However, the non-specific hydrophobic interactions permit the nanofiber to slide diffusion along the fiber in either direction that minimizes the exposure of hydrophobic alanines and eventually fill the gaps. The sliding diffusion phenomenon was also proposed for nucleic acids of polyA and polyU in 1956.[29,30] For clarity, these β-sheets are not presented as twisted strands. Color code: green, alanines; red, negatively charged amino acids; blue, positively charged amino acids (image courtesy of Hidenori Yokoi).

in early studies of nucleic acids where polyA and polyU form complementary base pairings that can slide diffuse along the double helical chains.[29,30] If however, the bases are heterogeneous, containing G, A, T, C, then the bases cannot undergo sliding diffusion. Likewise, if the hydrophobic side of the peptides does not always contain alanine, containing residues such as valine and isoleucine, it would become more difficult for sliding diffusion to occur due to their structural constraints.

On the charged side, both positive and negative charges are packed together through intermolecular ionic interactions in a checkerboard-like manner (looking from the top). Likewise, the collectively complementary + and − ionic interactions may also facilitate reassembly. Similar to restriction-digested DNA fragments, these nanofiber fragments could form various assemblies like blunt and protruding ends. The fragments with various protruding ends as well as blunt ends can reassemble readily through hydrophobic and ionic interactions (Fig. 8).

Designer peptides scaffold 3-D cell cultures

Although self-assembling peptides are promising scaffolds, they show no specific cell interaction because their sequences

are not naturally found in living systems. The next logical step is to directly couple biologically active and functional peptide motifs found in the literature. Accordingly, the second generation of designer scaffolds will have significantly enhanced interactions with cells and tissues.

For over 100 years, since the Petri dish was invented and used for tissue culture studies, almost all tissue cells have been studied on the 2D Petri dish and various formats of coated 2D surfaces. However, this 2D surface is rather unlike 3D tissue and the body's microenvironment. Thus it is important to develop a true 3D microenvironment to mimic the real tissue and body situation. The commonly used biomaterials are inadequate due to their microfiber and micropore size. Animal derived collagen gel and Matrigel contain other residue materials that are not always adequate for finely-controlled studies. Thus, a designer scaffold becomes more desirable.[37,38]

The simplest way to incorporate the functional motifs is to directly synthesize them by extending the motifs on to the self-assembling peptides themselves (Fig. 9). The functional motifs are coupled to the C-termini since solid phase peptide synthesis starts from C-termini. This helps avoid deletion during elongation synthesis (the longer the peptide extended from the C-termini, the more likely that there will be deletion errors). Usually a spacer comprising 2-glycine residues is added to guarantee flexible and correct exposure of the motifs to cell surface receptors. If one combines a few designer peptides with different active motifs, these different functional motifs in various ratios can be incorporated in the same scaffold (Fig. 9). Upon exposure to solution at neutral pH, the functionalized sequences self-assemble, leaving the added motifs on both sides of each nanofiber (Fig. 9). Nanofibers take part in the overall scaffold, thus providing functionalized microenvironments with specific biological stimuli (Fig. 9).

Self-assembling peptide scaffolds with functional motifs can be commercially produced at a reasonable cost. Thus, this method can be readily adopted for widespread uses including the study of cell interactions with their local- and micro-environments, cell migrations in 3D, tumor and cancer cells interactions with normal cells, cell processes and neurite extensions, cell based drug screen assays and other diverse applications.

We have produced different designer peptides from a variety of functional motifs with different lengths.[6–9] We showed that the addition of motifs in some cases to the self-assembling peptide RADA16-I did not significantly inhibit self-assembling properties. Furthermore, one can combine the RADA16-I nanofiber with the active designer self-assembling peptides by mixing the modified peptides. Although their nanofiber structures are indistinguishable from the RADA16-I scaffold, the appended functional motifs significantly influence cell behaviors.

Using the designer self-assembling peptide nanofiber system, every ingredient of the scaffold can be defined. Furthermore, it can be combined with multiple functionalities including soluble factors.[33] Cells reside in a 3-D environment where the extracellular matrix receptors on cell membranes can bind to the functional ligands appended to the peptide scaffolds. It is likely that higher tissue architectures with multiple cell types, rather than monolayers, could be constructed using these designer 3-D self-assembling peptide nanofiber scaffolds.

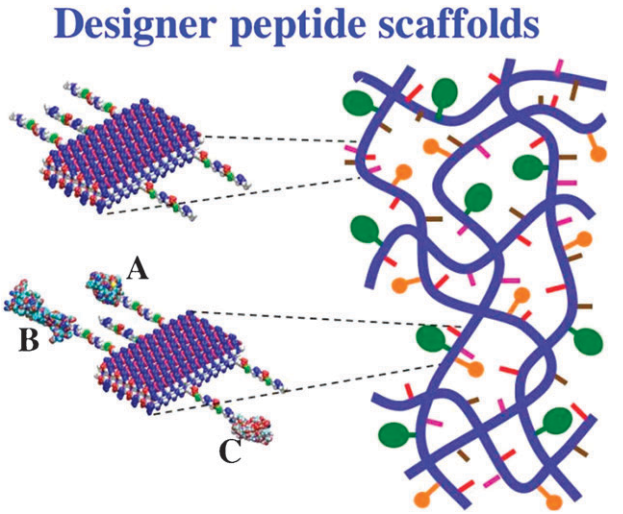

Fig. 9 Molecular and schematic models of the designer peptides and of the scaffolds. Direct extension of the self-assembling peptide sequence by adding different functional motifs. Light turquoise cylinders represent the self-assembling backbone and the yellow, pink, and tan lines represent various functional peptide motifs. Molecular model of a self-assembling peptide nanofiber with functional motifs flagging from both sides of the double β-sheet nanofibers. Either few or more functionalized and active peptide can be mixed at the same time. The density of these functionalized peptides can be easily adjusted by simply mixing them in various ratios, 1 : 1 to 1 : 1 000 000 or more before the assembling step. They then will be part of the self-assembled scaffold.

Even if only a fraction of functionalized motifs on the 3-D scaffold are available for cell receptor binding, cells may likely receive more external stimuli than when in contact with coated 2-D Petri dishes or RGD-coated (or other motifs) polymer microfibers, which is substantially larger than the cell surface receptors and in most cases, larger than the cells themselves. There, cells are not in a real 3-D environment, but rather, they are on a 2-D surface wrapping around the microfiber polymers with a curvature that depends on the diameter of the polymers. It is plausible in a 2-D environment, where only one side of the cell body is in direct contact with the surface, that receptor clustering at the attachment site may be induced; on the other hand, the receptors for growth factors, cytokines, nutrients and signals may be on the other sides that are directly exposed to the culture media. Perhaps cells may become partially polarized. In the 3-D environment, the functional motifs on the nanofiber scaffold surround the whole cell body in all dimensions. Thus growth factors may form a gradient in 3-D nanoporous microenvironments.

In our search for additional functional motifs, we found that a class of bone marrow homing peptides BMHP[7] is one of the most promising active motifs for stimulating adult mouse neural stem cell (NSC) adhesion and differentiation.[7] This observation suggests a new class of designer self-assembling peptides for 3-D cell biology studies.

Self-assembling peptide nanofiber scaffolds

Most polymer biomaterial fibers are many micrometres in diameter. The cells are attached to the microfibers with a

curvature. The scales of micro and nano differ by several orders of magnitude. The importance of nanoscale becomes obvious in 3-D cell cultures. It is clearly visible in the SEM images that the cells embedded in the self-assembling peptide nanofiber biological scaffolds are in a true 3-D environment (Fig. 9).[6–9] Here, the cells and cell clusters interact intimately with the extracellular matrix, which cells make on their own over time during cell growth and differentiation. Since the scaffolds are made mostly of water, ~99.0–99.5% water with 0.5%–1% peptide, cells can migrate freely without hindrance, just as fish swim freely in a seaweed forest.

Likewise, another self-assembling peptide, KLD12 (Ac-KLDLKLDLKLDL-NH_2), was used to culture primary bovine chondrocytes (Fig. 10).[22] The chondrocytes not only maintained their phenotype but also produced abundant type II collagen and glycosaminoglycan. Previously, it was known that chondrocytes dedifferentiate into fibroblast cell types and no longer produce type II collagen and glycosaminoglycans in coated 2D cell cultures. This showed the critical importance of 3D culture using a simple self-assembling peptide nanofiber scaffold.

These new self-assembling peptide nanofiber biological scaffolds have become increasingly important not only in studying 3-D spatial behaviors of cells, but also in developing approaches for a wide range of innovative medical technologies including regenerative medicine and controlled drug release (Fig. 11). One example is the use of peptide scaffolds to support neurite growth and differentiation, neural stem cell differentiation, cardiac myocytes, and bone and cartilage cell cultures. The peptide scaffolds from RADA16-I and RADA16-II formed nanofiber scaffolds in physiological solutions that stimulated extensive rat neurite outgrowth and active synapse formation on the peptide scaffold.[21] The peptide nanofiber scaffold has been injected into a hamster's brain to reconnect the severed optical track, which restored animal vision[31] because the peptide nanofiber scaffold encouraged abundant neural cell migration and high-density neuron synapses. This observation stimulated and inspired further experiments to directly repair the brain of animals. It may perhaps be possible to also repair various forms of human brain damage, stroke and aging after extensive clinical trial studies.

In addition, the same peptide nanofiber scaffold was also found to be a superb material for stopping bleeding in several tissues in only 10–20 s.[32] These examples are direct applications of self-assembling peptide materials to medical areas.

Additional experiments using skin cells also showed that the peptide scaffold stimulated keratinocyte and fibroblast migration in an *in vitro* wound healing model study.[33] This study suggests that the peptide scaffold may also be useful not only for skin wound care, but also useful for cosmetics to stimulate cell migration onto skin surface.

Designer self-assembling peptide nanofiber scaffolds for controlled molecular drug release

When one examines the peptide nanofiber scaffold under SEM and AFM, it is apparent that the self-assembling peptides form an ordered 3D scaffold with pores ranging from 5–200 nanometres.[3,6–9] The nanopore sizes are similar to the size of most small molecular drugs and therapeutic proteins. This observation suggests that scaffolds may be useful for controlled and sustained molecular release (Fig. 11).

When some small molecules were encapsulated in the peptide nanofiber scaffolds, these small molecules indeed released slowly depending on their characteristics.[34] These observations inspired us to directly encapsulate protein molecules since proteins are increasingly becoming effective therapeutics (for example, insulin and monoclonal antibodies).[35] The proteins showed a sustained release, mostly depending on the protein's molecular size and shape. The smaller proteins, such as lysozyme (molecular weight = 14 KDa), release faster than antibodies which are about 10 times larger (molecular weight = 150 KDa)[35] (Fig. 12).

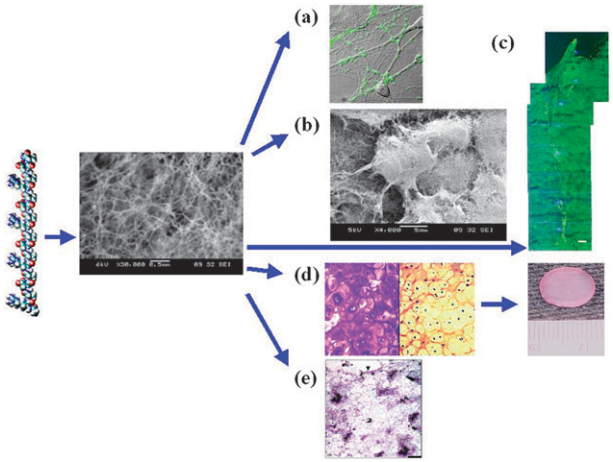

Fig. 10 From designer peptide to scaffold to tissues. (a) Active synapses on the peptide surface. Primary rat hippocampal neurons form active synapses on peptide scaffolds. The confocal images shown bright discrete green dot labeling indicative of synaptically active membranes after incubation of neurons with the fluorescent lipophilic probe FM-143. FM-143 can selectively trace synaptic vesicle turnover during the process of synaptic transmission. The active synapses on the peptide scaffold are fully functional, indicating that the peptide scaffold is a permissible material for neurite outgrowth and active synapse formation. (b) Adult mouse neural stem cells embedded in 3D scaffold (image courtesy of Fabrizio Gelain). (c) Brain damage repair in hamster. The peptide scaffold was injected into the optical nerve area of brain that was first severed with a knife (image courtesy of Rutledge Ellis-Behnke). The gap was sealed by the migrating cells after a few days. A great number of neurons form synapses. (d) Peptide KLD12 (KLDLKLDLKLDL), chondrocytes in the peptide scaffold and cartilage. The chondrocytes stained with TB showing abundant GAG production (left panel) and antibody to type II collagen demonstrating abundant Type II collagen production (right panel). A piece of pre-molded cartilage with encapsulated chondrocytes in the peptide nanofiber scaffold. The cartilage formed over a 3–4 week period after the initial seeding of the chondrocytes (image courtesy of John Kisiday). (e) Von Kossa staining showing transverse sections of primary osteoblast cells on HA-PHP-RADA16-I self-assembling peptide nanofiber scaffold. Scale bar = 0.1 mm. The intensely stained black areas represent bone nodules forming (image courtesy of Maria Bokhari).

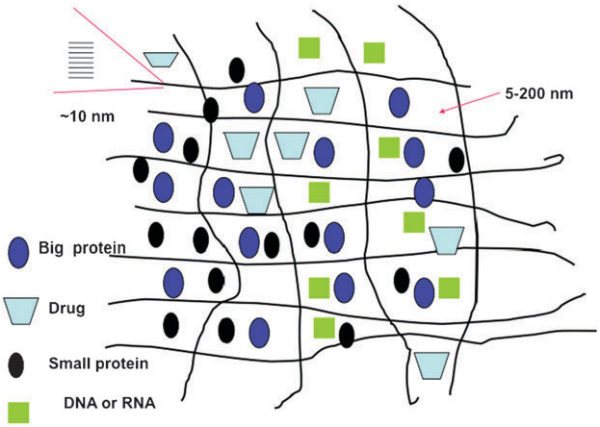

Fig. 11 Schematic illustration of the molecular releases from the designer self-assembling peptide nanofibers scaffolds. Stacked thin lines in the upper left represent the individual peptides. The black lines represent the peptide nanofibers. The drugs, proteins and DNA/RNA are represented by various shapes and colors embedded in the peptide nanofibers scaffold.

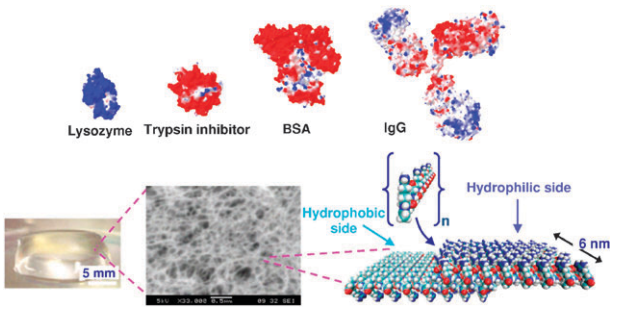

Fig. 12 Molecular representation of lysozyme, trypsin inhibitor, BSA, and IgG as well as of the ac-$(RADA)_4$-$CONH_2$ peptide monomer and of the peptide nanofiber. Color scheme for proteins and peptides: positively charged (blue), negatively charged (red), hydrophobic (light blue). Protein models were based on known crystal structures.

Furthermore, the release profiles can be fine-tuned since lower concentrations of peptides form lower density nanofiber scaffolds, which have larger pores. On the other hand, higher concentrations of peptide form higher density nanofiber scaffolds, which have smaller pores (Fig. 13).

In an analogy, the movement of particles through the scaffold can be compared to a rabbit running through grass. If amplifying the nanofiber (~5 nanometres in diameter) 10 million times, the dimension is similar to a single blade of grass (to 5 millimetres). A rabbit in the grassland runs at different speeds due to the hindrance of the grass density. The denser the grass, the slower the rabbit moves (higher concentration of scaffold). The less dense the grass, the faster the rabbit can run.

Chen Pu and his colleagues also used peptide scaffolds to encapsulate the hydrophobic anticancer drug ellipticine.[36] They showed that the peptides stabilized the drug and increased its efficacy since the non-stabilized ellipticine degraded quickly, thus losing its potency. One of the peptides, EFK16-IIs stabilized neutral ellipticine molecules and ellipticine microcrystals.[36] Since many anticancer drugs are either not water-soluble or are unstable in water, their findings could be further developed for effective anticancer drug delivery.

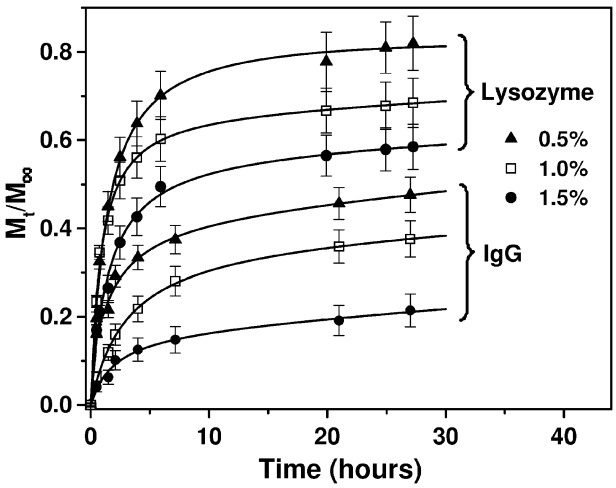

Fig. 13 The release profiles for lysozyme and IgG through hydrogels of different peptide nanofiber densities. Hydrogels consisted of self-assembling peptide ac-$(RADA)_4$-$CONH_2$ with concentrations of 0.5% w/v (filled triangles), 1.0% w/v (hollow squares), and 1.5% w/v (filled circles). Release experiments were performed in PBS, pH 7.4 at room temperature. Data points represent the average of 5 samples with calculated standard deviations less than 12%.

Designer peptide scaffolds for bone cells and 3-D migration

The designer self-assembling peptide nanofiber scaffolds have been shown to be an excellent biological material for 3-D cell cultures and to be capable of stimulating cell migration into the scaffold.[8,9] We developed several peptide nanofiber scaffolds designed specifically for osteoblasts.[8] We designed one of the pure self-assembling peptide scaffolds, RADA16-I, through direct coupling to short biologically active motifs. The motifs included osteogenic growth peptide ALK (ALKRQGRTLYGF) bone-cell secreted-signal peptide, osteopontin cell adhesion motif DGR (DGRGDSVAYG) and 2-unit RGD binding sequence PGR (PRGDSGYRGDS). The new peptide scaffolds are made by mixing the pure RADA16-I and designer peptide solutions, and the molecular integration of the mixed nanofiber scaffolds was examined using AFM. Compared to pure RADA16-I scaffold, it was found that these designer peptide scaffolds significantly promoted mouse pre-osteoblast MC3T3-E1 cell proliferation. Moreover, alkaline phosphatase (ALP) activity and osteocalcin secretion, which are early and late markers for osteoblastic differentiation, were also significantly increased, thus demonstrating that the designer, self-assembling peptide scaffolds promoted the proliferation and osteogenic differentiation of MC3T3-E1.

Under identical culture medium conditions, confocal images unequivocally demonstrated that the designer PRG peptide scaffold stimulated cell migration into the 3D scaffold (Fig. 14).[7,8] Without the modified active motif, cells stayed in the same scaffold. These observations will likely stimulate further research studying cell migration in 3D under well-defined conditions since the designer scaffolds can be fine-tuned and

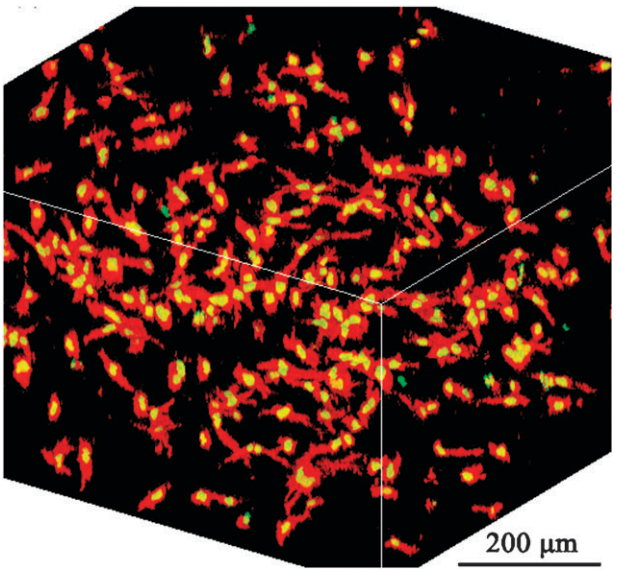

Fig. 14 A laser confocal scanning microscopy image of human endothelial cell 3D migration. It shows that the cell migrated several hundred micrometres into the peptide scaffold. The 3D culture system is more realistic for real body 3D environment, in sharp contrast to the conventional 2D artificial culture system (image courtesy of Akihiro Horii and Xiumei Wang).

well controlled. This is in sharp contrast to current cell culture conditions using collagens and Matrigel that contain unknown ingredients and thus make it difficult to reproduce experimental results. Fig. 15

Collagen production without extra addition of soluble growth factors

Extracellular matrix protein production is crucial for regenerative medicine and tissue engineering. If cells are provided with a hospitable environment, cells typically produce their own extracellular matrix proteins, including various collagens. Most current studies have focused on using soluble growth factors to stimulate extracellular matrix protein (including collagen) production. However, we have demonstrated that designer peptide scaffolds containing the active motifs of 2-unit RGD binding sequence PRG (PRGDSGYRGDS) and laminin cell adhesion motif PDS (PDSGR) can equally stimulate production of collagen without extra addition of soluble growth factors. RGD and laminin have been previously shown to promote specific biological activities including periodontal ligament fibroblasts adhesion, proliferation and protein production. Compared to the pure RADA16 peptide scaffold, we here show that these designer peptide scaffolds significantly promote human periodontal ligament fibroblasts to proliferate and migrate into the scaffolds (for ~300 μm in 2 weeks). Moreover these peptide scaffolds significantly stimulated periodontal ligament fibroblasts to produce extracellular matrix proteins without using extra additional growth factors. Immunofluorescent images clearly demonstrated that the cells embedded in the peptide scaffolds were almost completely covered with type I and type III collagens (Fig. 16), which are the main protein components of periodontal ligaments. These results

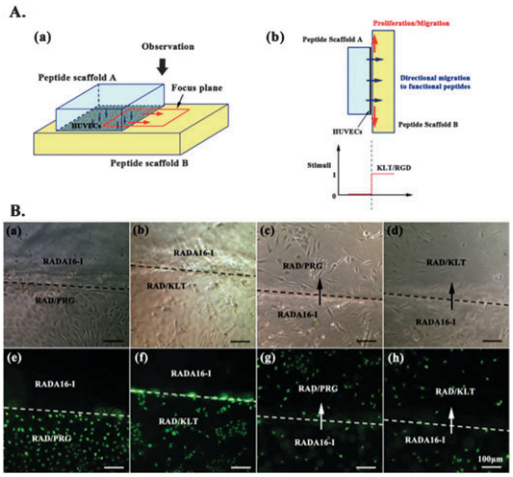

Fig. 15 Human endothelial cell unidirectional migration in responding to functionalized peptide scaffolds. (A) Schematic illustrations of cell directional migration. (a) Clear-boundary-sandwich cell migration assay. (b) Directional migration induced by functional motifs. (B) Phase contrast microscopy images of HUVECs seeded on peptide scaffolds: (a) RAD/PRG; (b) RAD/KLT; (c) and (d) RADA16-I, and fluorescent SYTOX green nuclear staining for (e) RAD/PRG; (f) RAD/KLT; (g) and (h) RADA16-I. Cells directionally migrated from RADA16-I to RAD/PRG (c and g) and RAD/KLT (d and h). The scale bar is 100 μm for all panels (image courtesy of Xiumei Wang).

suggest that these designer self-assembling peptide nanofiber scaffolds may be useful for promoting wound healing, especially periodontal ligament tissue regeneration, without the addition of extra growth factors. Beyond accelerating wound healing, stimulation of various collagen productions without soluble growth factors may also have implications in the cosmetic field. If we can design cream and hydrogel materials that can

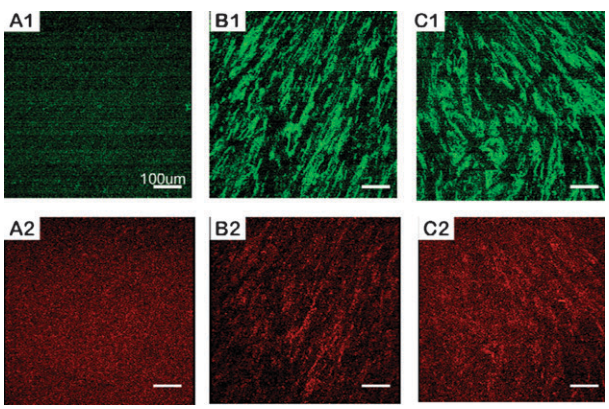

Fig. 16 Type I and Type III Collagens production without extra addition of soluble growth factors from periodontal ligament fibroblasts. The fluorescent immunostaining images of periodontal ligament fibroblasts on the different scaffolds after a 6 week culture. Fluorescent immunostaining with Anti-collagen type I and Alexa fluor-488 goat anti-rabbit IgG for collagen type I (green) in (A1) RADA16, (B1) PRG and (C1) PDS. PDS, and Anti-collagen type III and Alexa fluor 594 goat anti-mouse IgG for collagen type III (red) in (A2) RADA16, (B2) PRG and (C2) PDS. The ratio of designer PRG/PDS to RADA16 scaffold is 1 : 9. The scale bar represents 100 μm for all images (image courtesy of Yoshiyuki Kumada).

stimulate collagen production, it may facilitate skin to produce collagens thus regenerating youthful skin texture.

Designer self-assembling peptide nanofiber scaffolds for reparative, regenerative medicine and tissue engineering

Designer self-assembling peptide nanofiber scaffolds have a wide spectrum of uses in addition to 3D cell culture. Bokhari and colleagues in the UK produced a peptide hydrogel–polyHIPE polymer hybrid material to enhance osteoblast growth and differentiation.[39] Richard Lee and his colleagues at Harvard Medical School used the scaffolds to promote angiogenesis.[40] When they injected the scaffold into mouse heart muscle, the peptide nanofibers created intramyocardial microenvironments for endothelial cells.[41] Moreover, they also showed that the local myocardial IGF-1 delivery with biotinylated peptide nanofibers improved cell therapy for myocardial infarction in mice.[42] These studies suggest the peptide scaffolds may be useful in the future for healthcare technology.

As time progresses, more and more regenerative medicine studies and clinical trials using the designer peptide nanofiber scaffolds will likely become available.

Concluding remarks

Leonardo da Vinci stated over 550 years ago "When nature finishes to produce its own species, man begins using natural things in harmony with this very nature to create an infinity of species". Although we have created many molecular species using natural amino acids, there is no doubt that infinitely more will come.

Susan Lindquist of MIT also said eloquently, "About 10 000 years ago, humans began to domesticate plants and animals. Now it's time to domesticate molecules". Indeed, we are just at the beginning of domesticating and designing numerous completely new molecules and new biological materials with defined and desired functionalities.

Human civilizations are usually divided according to the materials that dominate in the society: the Stone Age, the Bronze Age, the Iron Age, the Plastic age and the Silicon age. The new designer materials age is now upon us. The designer biological materials space is wide open and limited only by our imaginations.

References

1 S. Zhang, C. Lockshin, A. Herbert, E. Winter and A. Rich, *EMBO. J.*, 1992, **11**, 3787–3797.
2 S. Zhang, T. Holmes, C. Lockshin and A. Rich, *Proc. Natl. Acad. Sci. U. S. A.*, 1993, **90**, 3334–3338.
3 S. Zhang, C. Lockshin, R. Cook and A. Rich, *Biopolymers*, 1994, **34**, 663–672.
4 S. Zhang, *Biotechnol. Adv.*, 2002, **20**, 321–339.
5 S. Zhang, T. Holmes, M. DiPersio, R. O. Hynes, X. Su and A. Rich, *Biomaterials*, 1995, **16**, 1385–1393.
6 S. Zhang, F. Gelain and X. Zhao, *Semin. Cancer Biol.*, 2005, **15**, 413–420.
7 F. Gelain, D. Bottai, A. Vescovi and S. Zhang, *PLoS One*, 2006, **1**, e119.
8 A. Horii, X. M. Wang, F. Gelain and S. Zhang, *PLoS One*, 2007, **2**, e190.
9 X. Wang, A. Horii and S. Zhang, *Soft Matter*, 2008, **4**, 2388–2395.
10 S. Zhang and A. Rich, *Proc. Natl. Acad. Sci. U. S. A.*, 1997, **94**, 23–27.
11 M. Altman, P. Lee, A. Rich and S. Zhang, *Protein Sci.*, 2000, **9**, 1095–1105.
12 S. Zhang, L. Yan, M. Altman, M. Lässle, H. Nugent, F. Frankel, D. Lauffenburger, G. M. Whitesides and A. Rich, *Biomaterials*, 1999, **20**, 1213–1220.
13 S. Vauthey, S. Santoso, H. Gong, N. Watson and S. Zhang, *Proc. Natl. Acad. Sci. U. S. A.*, 2002, **99**, 5355–5360.
14 S. Santoso, W. Hwang, H. Hartman and S. Zhang, *Nano Lett.*, 2002, **2**, 687–691.
15 G. von Maltzahn, S. Vauthey, S. Santoso and S. Zhang, *Langmuir*, 2003, **19**, 4332–4337.
16 S. J. Yang and S. Zhang, *Supramol. Chem.*, 2006, **18**, 389–396.
17 A. Nagai, Y. Nagai, H. Qu and S. Zhang, *J. Nanosci. Nanotechnol.*, 2007, **7**, 2246–2252.
18 U. Khoe, Y. L. Yang and S. Zhang, *Macromol. Biosci.*, 2008, **8**, 1060–1067.
19 U. Khoe, Y. L. Yang and S. Zhang, *Langmuir*, 2009, **25**, 4111–4114.
20 M. Caplan, E. Schwartzfarb, S. Zhang, R. D. Kamm and D. A. Lauffenburger, *Biomaterials*, 2002, **23**, 219–227.
21 T. Holmes, S. Delacalle, X. Su, A. Rich and S. Zhang, *Proc. Natl. Acad. Sci. U. S. A.*, 2000, **97**, 6728–6733.
22 J. Kisiday, M. Jin, B. Kurz, H. Hung, C. Semino, S. Zhang and A. J. Grodzinsky, *Proc. Natl. Acad. Sci. U. S. A.*, 2002, **99**, 9996–10001.
23 S. Zhang and M. Altman, *React. Funct. Polym.*, 1999, **41**, 91–102.
24 D. Marini, W. Hwang, D. Lauffenburger, S. Zhang and R. D. Kamm, *Nano Lett.*, 2002, **2**, 295–299.
25 H. Yokoi, T. Kinoshita and S. Zhang, *Proc. Natl. Acad. Sci. U. S. A.*, 2005, **102**, 8414–8419.
26 L. Pauling, *Nature of the Chemical Bond and the Structure of Molecules and Crystals: An Introduction to Model Structural Chemistry*, Cornell Univ. Press, Ithaca NY, 3rd edn, 1960.
27 Z. Luo, X. Zhao and S. Zhang, *PLoS One*, 2008, **3**, e2364.
28 Z. Luo, X. Zhao and S. Zhang, *Macromol. Biosci.*, 2008, **8**, 785–791.
29 A. Rich and D. R. Davies, *J. Am. Chem. Soc.*, 1956, **78**, 3548–3549.
30 G. Felsenfeld and D. R. Davies, *J. Am. Chem. Soc.*, 1957, **79**, 2023–2024.
31 R. G. Ellis-Behnke, Y. X. Liang, S. W. You, D. Tay, S. Zhang, K. -F. So and G. Schneider, *Proc. Natl. Acad. Sci. U. S. A.*, 2006, **103**, 5054–5059.
32 R. G. Ellis-Behnke, Y. X. Liang, D. K. C. Tay, P. W. F. Kau, G. E. Schneider, S. Zhang, W. Wu and K. -F. So, *Nanomed.: Nanotechnol., Biol. Med.*, 2006, **2**, 207–215.
33 A. Schneider, J. A. Garlick and C. Egles, *PLoS One*, 2008, **3**, e1410.
34 Y. Nagai, L. D. Unsworth, S. Koutsopoulos and S. Zhang, *J. Controlled Release*, 2006, **115**, 18–25.
35 S. Koutsopoulos, L. D. Unsworth, Y. Nagai and S. Zhang, *Proc. Natl. Acad. Sci. U. S. A.*, 2009, **106**, 4623–4628.
36 S. Y. Fung, H. Yang and P. Chen, *PLoS One*, 2008, **3**, e1956.
37 S. Zhang, *Nat. Biotechnol.*, 2003, **21**, 1171–1178.
38 S. Zhang, *Nat. Biotechnol.*, 2004, **22**, 151–152.
39 M. A. Bokhari, G. Akay, S. Zhang and M. A. Birch, *Biomaterials*, 2005, **26**, 5198–5208.
40 D. A. Narmoneva, O. Oni, A. L. Sieminski, S. Zhang, J. P. Gertler, R. D. Kamm and R. T. Lee, *Biomaterials*, 2005, **26**, 4837–4846.
41 M. E. Davis, J. P. M. Motion, D. A. Narmoneva, T. Takahashi, D. Hakuno, R. D. Kamm, S. Zhang and R. T. Lee, *Circulation*, 2005, **111**, 442–450.
42 M. E. Davis, P. C. H. Hsieh, T. Takahashi, Q. Song, S. Zhang, R. D. Kamm, A. J. Grodzinsky, P. Anversa and R. T. Lee, *Proc. Natl. Acad. Sci. U. S. A.*, 2006, **103**, 8155–8160.

